

Silver nanowire array infrared polarizers

This article has been downloaded from IOPscience. Please scroll down to see the full text article.

2003 Nanotechnology 14 20

(<http://iopscience.iop.org/0957-4484/14/1/305>)

View [the table of contents for this issue](#), or go to the [journal homepage](#) for more

Download details:

IP Address: 61.190.88.136

The article was downloaded on 09/01/2013 at 01:57

Please note that [terms and conditions apply](#).

Silver nanowire array infrared polarizers

Y T Pang¹, G W Meng, Q Fang and L D Zhang

Institute of Solid State Physics, Chinese Academy of Sciences, PO Box 1129, Hefei 230031, Peoples' Republic of China

E-mail: ytpang@263.net

Received 12 August 2002, in final form 30 October 2002

Published 3 December 2002

Online at stacks.iop.org/Nano/14/20

Abstract

A silver nanowire array micropolarizer within an anodic alumina membrane (AAM) was fabricated by anodization of pure Al foil and electrodeposition of Ag, respectively. X-ray diffraction, scanning electron microscopy, and transmission electron microscopy investigations reveal that the nanowires are essentially single crystals, and have an average diameter of 90 nm. Spectrophotometer measurements show that the silver nanowire arrays embedded in the AAM can only transmit vertically polarized light to the wires. An extinction ratio of 25–26 dB and average insertion loss of 0.77 dB in the wavelength range 1–2.2 μm were obtained, respectively. Therefore the Ag nanowire/AAM can be used as a wire-grid type polarizer.

1. Introduction

Polarization is one of the most important factors which affects the performance of optical devices such as isolators, switches and junctions. Recent progress in optical communications has promoted improvement and miniaturization of these devices, and accordingly there is strong demand for small, rugged and highly efficient polarizing elements. Although many kinds of polarizers such as pile-of-plates, dichroic sheet and wire-grid polarizers have already been developed [1–6], the bulkiness of these polarizers or high fabrication cost has limited their applications. Using alumina and nickel by means of anodization and electrodeposition techniques, Miyagi *et al* [7] recently proposed novel optical elements. It is well known that the anodic alumina membrane (AAM) consists of numerous parallel cylindrical channels. Consequently, the AAM shows anisotropic optical properties. When metallic materials are filled in the channels, the metal/AAM film will act as a wire-grid polarizer. It is expected that the film will be superior to conventional polarizing elements with respect to efficiency and compactness as well as in terms of fabrication cost [8]. Nevertheless, in the process of Miyagi's experiment, the aluminium film was anodized in a solution of sulfuric acid only once. The order of the channels in the AAM obtained using this anodizing process was not uniform. On the other hand, in their experiment the optical properties of the polarizer were only demonstrated for two wavelengths: 1.3 and 0.63 μm [7].

Silver nanowires or nanorods have been recently prepared and studied by several groups [9–12] because of their

potential applications in microelectronics, optical, electronic and magnetic devices. Here, we present a method developed to fabricate a silver nanowire micropolarizer within the nanochannels of the AAM, and the optical properties of the micropolarizer are presented over a wide wavelength region of 1–2.2 μm .

2. Experimental details

The through-hole AAM with ordered nanochannels was prepared via a two-step anodization process as described in detail elsewhere [13–18]. The first anodization was conducted under a constant voltage of 40 V at 5 °C in oxalic acid, in a thermally isolated electrochemical cell for 4 h, during which the electrolyte was vigorously stirred using a pump system. Then the alumina layer produced was removed by wet chemical etching in a mixture of phosphoric acid (6 wt%) and chromic acid (1.8 wt%) at 60 °C for 6 h. The second anodization process was carried out under the same conditions as those used in the first. After coating a protecting layer on the surface of the porous alumina film, the central aluminium substrate was removed in a saturated HgCl_2 solution, and the surrounding aluminium was retained as a support. Subsequent etching treatment was carried out in a 6 wt% phosphoric acid solution at 30 °C for 70 min to remove the barrier layer on the bottom side of the AAM. A layer of gold was sputtered onto one side of the AAM to serve as the working electrode in a two-electrode electrochemical cell. The electrolyte contained a mixture of 300 g l⁻¹ AgNO_3 and 45 g l⁻¹ H_3BO_3 solutions and was buffered to pH = 2.5 with nitric acid.

¹ Author to whom any correspondence should be addressed.

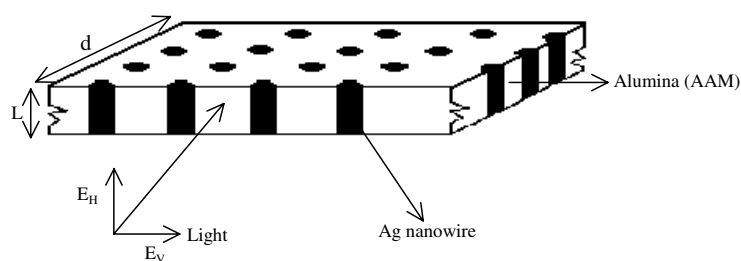


Figure 1. Schematic illustration of the Ag/AAM sample. A film was sliced to a thickness of $d = 10 \mu\text{m}$, and the sliced surfaces were polished. The direction of polarization is designated as H- or V-polarization depending upon whether the electric field of the light is horizontal or vertical to the nanowires.

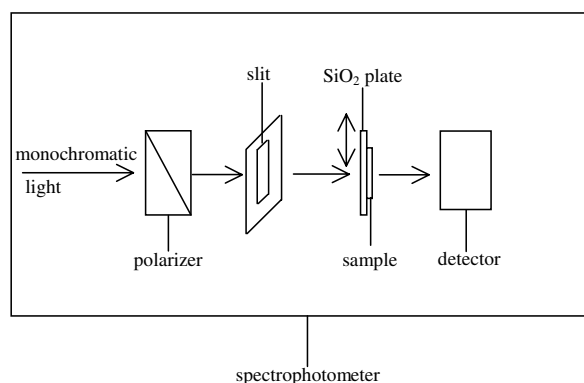


Figure 2. The experimental set-up used for the evaluation of the optical loss. The sample and the SiO_2 glass plate can be moved up and down (see the double arrow) by a micromechanical stage.

The electrodeposition was carried out for 10 h at a constant current density (2.5 mA cm^{-2}), with graphite serving as the counter electrode at room temperature.

The Ag nanowire arrays embedded in the AAM were characterized by an x-ray diffractometer (XRD MXP18AHF) (D/Max-rA) with $\text{Cu K}\alpha$ radiation ($\lambda = 1.5405 \text{ \AA}$) and scanning electron microscopy ((SEM) JEOL JSM-6300). Transmission electron microscopy ((TEM) JEM-200CX) and selected-area electron diffraction (SAED) were employed to characterize the individual Ag nanowires. For SEM observation, a piece of AAM embedded with Ag nanowires was eroded in 5% NaOH solution at 30°C for 30 min to partially remove the AAM and then attached to the SEM stub after careful rinsing with deionized water. A thin gold layer was evaporated to form a conducting film for observation. For TEM observation, a small piece of Ag/AAM was placed in the same solution for SEM observation for 60 min to remove the AAM completely. The solution was then slowly removed using a syringe and was carefully replaced with distilled water to rinse the products. The rinsing process was repeated three times. The remaining black solid was collected and ultrasonically dispersed in 1 ml of ethanol. A drop of solution was placed on a carbon grid and allowed to dry prior to electron microscope analysis. For optical measurement, a portion of the sample was sliced off and the cross-sectional surfaces were polished until the thickness (d) became as thin as $\sim 10 \mu\text{m}$ (see figure 1). The length (L) of the sample was $\sim 60 \mu\text{m}$ (see figure 1). The prepared sample was stuck

onto a SiO_2 glass plate for mechanical support in the optical measurement. The optical loss of the sample was evaluated using a spectrophotometer (Cary 5E) and the experimental set-up is shown in figure 2. The sample was positioned on a rotating stage so that the direction of polarization could be either horizontal (H polarization) or vertical (V polarization) with respect to the nanowires. The infrared light (from 1 to $2.2 \mu\text{m}$) was transmitted through a polarizer prism and a narrow slit and reached the sample at normal incidence.

3. Results and discussion

The x-ray diffraction pattern of the prepared Ag/AAM sample is shown in figure 3. The broad peak resulting from the AAM indicates that the AAM is amorphous. The four peaks are found to be very close to (111), (200), (220) and (311) of bulk Ag, indicating that the face-centred cubic (fcc) structure of bulk Ag is preserved in these wires. Figure 4 shows the SEM images of the Ag nanowire arrays prepared in the AAM template. It can be seen that large quantities of Ag nanowires with high packing density have been fabricated. The TEM image of the prepared sample (figure 5(a)) shows a number of nanowires with an average diameter of about 90 nm, which is nearly equal to the channel diameters of the AAM used. A TEM image of a single nanowire is shown in figure 5(b). The SAED pattern taken from this nanowire corresponds with that of Ag (figure 5(c)).

The optical transmission of the Ag/AAM sample (figure 6(a)) was obtained using the spectrophotometer (figure 2). The light intensity transmitted only through the SiO_2 glass plate without a sample was also measured as a reference (curve B). Curves H and V denote the transmittance of horizontal and vertical incident light, respectively. Curve H was amplified 40 times for clear display. The transmission difference between H and V demonstrates prominent optical anisotropy of the sample, i.e. optical transmission increases significantly when the direction of polarization is changed from horizontal to vertical to the nanowires.

Figure 6(b) shows the optical loss of the sample calculated from the transmittance with and without the Ag/AAM sample. Concretely, curve L_h (figure 6(b)) was calculated from the light intensity ratio of B to H. Therefore, curve L_h presents the extinction ratio (i.e. the loss for horizontal polarization). Curve L_v (figure 6(b)) was calculated from the light intensity ratio of B to V. Consequently, curve L_v presents the insertion loss (i.e. the

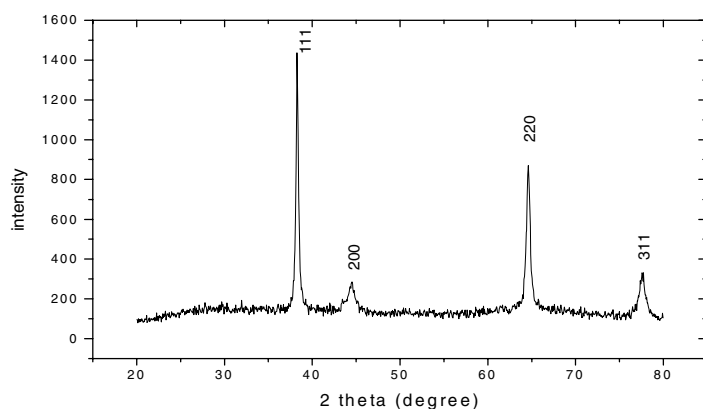


Figure 3. XRD spectrum of the Ag nanowire arrays embedded in the AAM.

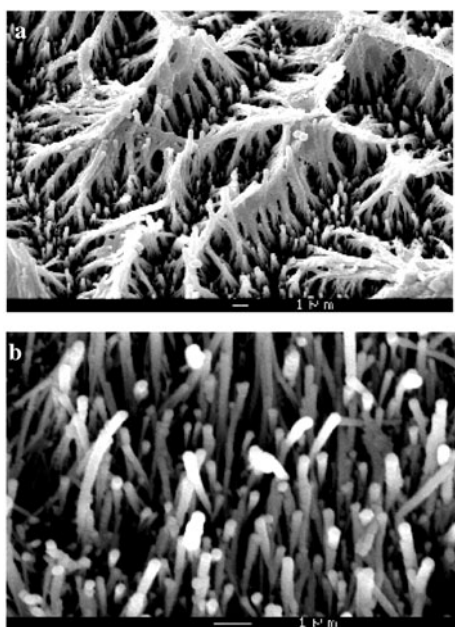


Figure 4. SEM images of the ordered Ag nanowire arrays: (a) low-magnification image; (b) high-magnification image.

loss for vertical polarization). In the whole wavelength region applied, there is a great difference in optical loss between L_h and L_v . For example, at the wavelength of $2.2 \mu\text{m}$, the insertion loss is only 0.5 dB and the extinction ratio is as large as 26 dB. As the wavelength becomes longer, the extinction ratio increases, whereas the insertion loss decreases, which is in agreement with the theoretical prediction [8].

The curves L_h and L_v presented in figure 6(b) reveal the polarizing function of the sample, i.e. the extinction ratio of 25–26 dB and average insertion loss of 0.77 dB in the wavelength region of 1– $2.2 \mu\text{m}$, respectively. The extinction ratio is smaller than the expected values [8]. One possible reason may be the defects in the silver nanowires. The electrochemical deposition process could be improved to fabricate defect-free nanowires. Other possible reasons for the discrepancies between experimental values and theoretical analysis are as follows: variation of the nanowire density, oxidation of the metal Ag nanowires. The large insertion loss of the sample seems to originate mainly from the scattering in the sample

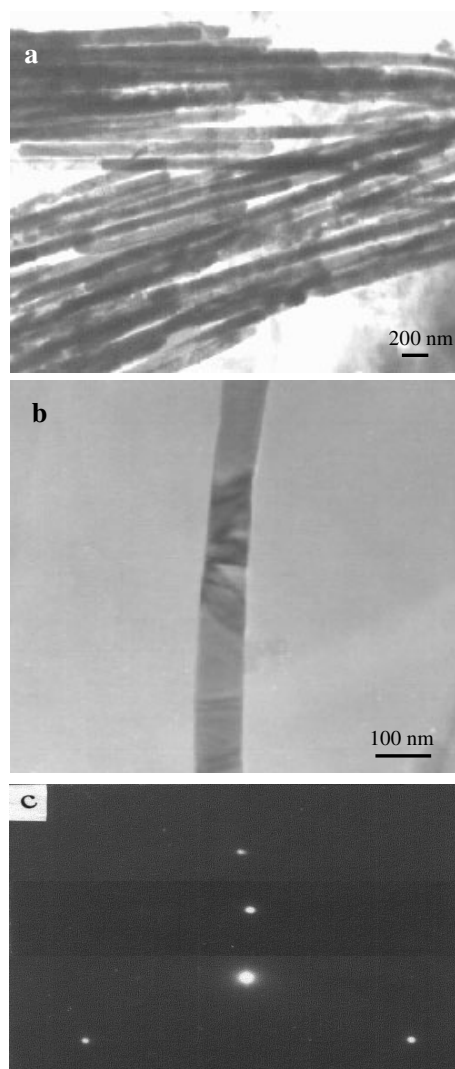


Figure 5. (a) TEM image of Ag nanowires after removing the AAM. (b) and (c) TEM image and SAED pattern from an individual nanowire.

surfaces. The scattering can be attributed to the roughness of the polished surfaces.

To investigate the homogeneity of the transmission of the sample, we measured the optical transmission of the

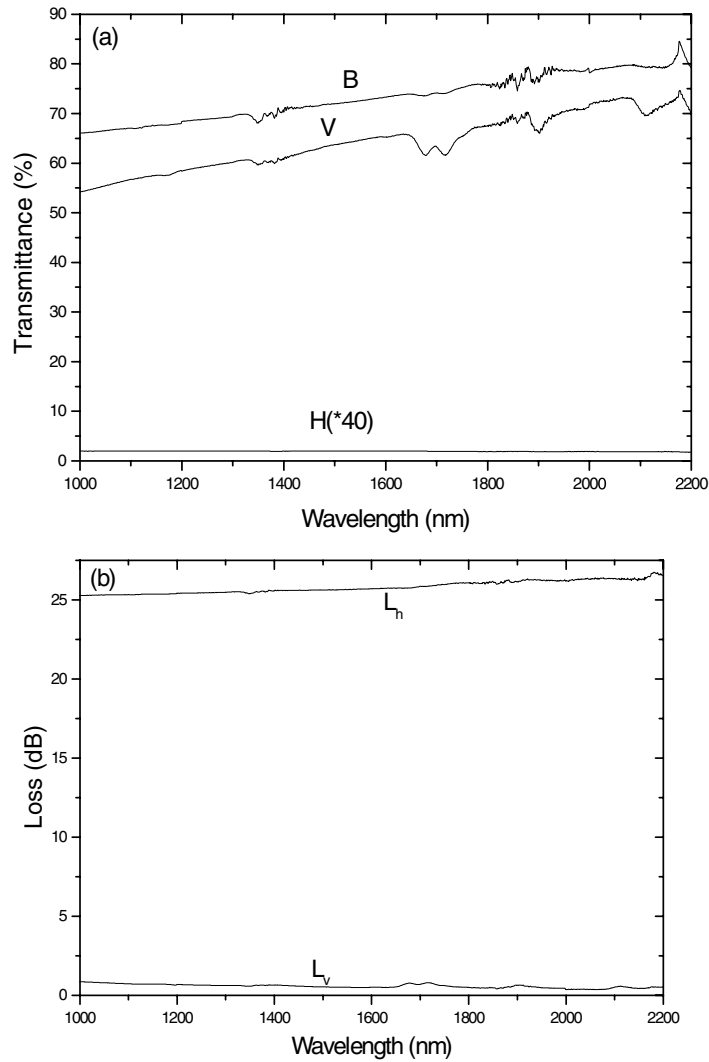


Figure 6. Transmission (a) and optical loss (b) of silver nanowire arrays embedded in the AAM measured in the wavelength region 1 to 2.5 μm . In (a) curve B expresses the transmission of incident light that only passes through the silica substrate, curves H and V express the transmission of incident light that passes through both the silica and sample, horizontally and vertically to the nanowires, respectively. Curve H was amplified 40 times for clear display. In (b) curves L_h and L_v express the extinction ratio and insertion loss calculated from (a), respectively. The film thickness is about 10 μm .

sample by moving the sample up and down slightly with a micromechanical stage (see the double arrows in figure 2). The results are shown in figure 7. It can be seen that the transmissions of V and H are slightly different from their counterparts shown in figure 6(a). The inhomogeneity of the transmission of the sample is due to the non-uniformity of the sample thickness.

To evaluate the Ag nanowire polarizer arrays embedded in the AAM for practical application, we compare it with two popular commercial polarizers, i.e. the conventional wire grid and the Glan–Thompson prism. The extinction ratio and the insertion loss presented in figure 6(b) show a more efficient polarizer than those of the conventional wire grids [19–21], because the performance of a wire-grid polarizer is determined by the wire size. To attain a high extinction ratio and low insertion loss, the diameter of the Ag nanowire and the spacing between the wires must be sufficiently smaller than the wavelength of incident light. Since conventional wire grids are fabricated by photolithography, the wire size cannot

be made small enough, and consequently the performance becomes poor in comparison with silver nanowires embedded in the AAM. The Glan–Thompson prism has an excellent polarization property from visible to near infrared. However, they are made of calcite crystals and are rather expensive to produce. Although the polarization of the sample is inferior to the Glan–Thompson prism at present, the Ag/AAM polarizer has the advantage for practical applications from the viewpoint of fabrication cost.

4. Conclusion

In conclusion, a micropolarizer was achieved by using ordered Ag nanowire arrays embedded in the AAM. XRD and TEM investigation results indicate that the single crystalline Ag nanowires were uniformly assembled into the ordered channels of the anodic alumina. Spectrophotometric measurement reveals that nanoscopic metal in the channels gives rise to a large loss for the horizontal polarization but not for the vertical

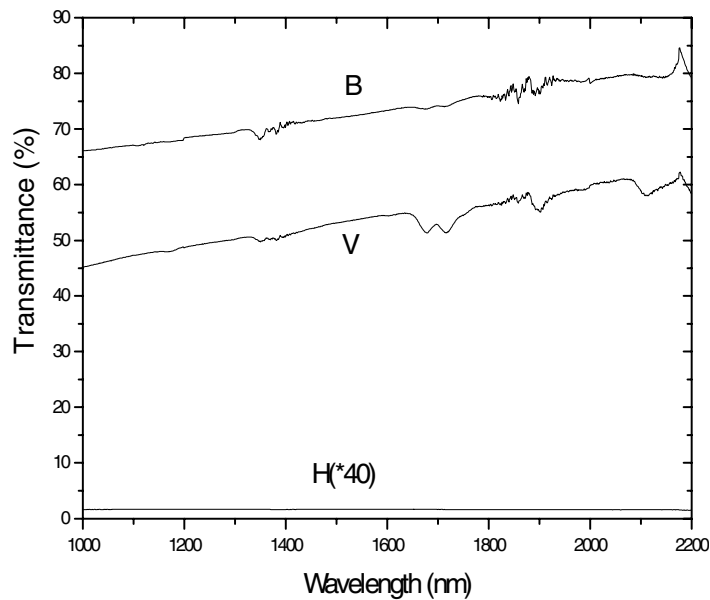


Figure 7. Optical transmission of the Ag/AAM sample measured in different areas compared with figure 5.

polarization to the wires. With the micropolarizer, we attained an extinction ratio of 25–26 dB and an average insertion loss of 0.77 dB in the whole wavelength range 1–2.2 μm , respectively. Therefore, silver nanowires embedded in the AAM would be an attractive optical element in the IR spectral region, where an efficient and cheap polarizer is not currently available.

Acknowledgments

The authors would like to express their appreciation to Professor Yongbang Yao and Junhui Jia for their fruitful discussions. This work was funded by the National Major Project of Fundamental Research: the Ministry of Sciences and Technology of China and the Natural Science Foundation of China (grant no 19974055).

References

- [1] Bird G R and Schurcliff W A 1959 *J. Opt. Soc. Am.* **49** 235
- [2] Yang J B, Graham H A and Peterson E W 1965 *Appl. Opt.* **4** 1023
- [3] Rupprecht G, Ginsberg D M and Leslie J D 1962 *J. Opt. Soc. Am.* **52** 665
- [4] Yokogawa T, Ogura M and Ajiwara T K 1988 *Appl. Phys. Lett.* **52** 120
- [5] Suchoski P G, Findakly T K and Leonberger F J 1988 *Opt. Lett.* **13** 172
- [6] Baba K, Shiraishi K, Obi K, Ataoka T K and Kawakami S 1988 *Appl. Opt.* **27** 2554
- [7] Saito M, Kirihara M, Taniguchi T and Miyagi M 1989 *Appl. Phys. Lett.* **55** 607
- [8] Saito M and Miyagi M 1989 *Appl. Opt.* **28** 3529
- [9] Braun E, Eichen Y, Sivan U and Ben-Yoseph G 1998 *Nature* **391** 775
- [10] Huang M H, Choudrey A and Yong P D 2000 *Chem. Commun.* 1063
- [11] Sloan J, Wright D M, Woo H-G, Bailey S, Brown G, York A P E, Coleman K S, Huchison J L and Green M L H 1999 *Chem. Commun.* 699
- [12] Govindaraj A, Satishkumar B C, Nath M and Rao C N R 2000 *Chem. Mater.* **12** 202
- [13] Masuda H, Yada K and Osaka A 1998 *Japan. J. Appl. Phys.* **37** L1340
- [14] Li A P, Müller F, Birner A, Nielsch K and Gösele U 1999 *Adv. Mater.* **11** 483
- [15] Jessensky O, Müller F and Gösele U 1998 *J. Electrochem. Soc.* **145** 3735
- [16] Jessensky O, Müller F and Gösele U 1998 *Appl. Phys. Lett.* **72** 1173
- [17] Masuda H, Hasegawa F and Ono S 1997 *J. Electrochem. Soc.* **144** L127
- [18] Li A P, Müller F, Birner A, Nielsch K and Gösele U 1998 *J. Appl. Phys.* **84** 6023
- [19] Auton J P 1967 *Appl. Opt.* **6** 1023
- [20] Cheo P K and Bass C D 1971 *Appl. Phys. Lett.* **18** 565
- [21] Auton J P and Hutley M C 1972 *Infrared Phys.* **12** 95